Supplementary Material

Sekikaic acid modulates the pancreatic β-cells in Streptozotocin-induced type 2 diabetic rats by inhibiting digestive enzymes

Vinay Bharadwaj Tatipamula[a,b]*, Satya Sowbhagya Priya Annam[c], Ha Thi Nguyen[a,d], Haritha Polimati[c], and Rajendra Prasad Yejella[c]

[a]Institute of Research and Development, Duy Tan University, Da Nang 550000, Vietnam; [b]Faculty of Pharmacy, Duy Tan University, Da Nang 550000, Vietnam; [c]Pharmaceutical Sciences Department, University College of Pharmaceutical Sciences, Andhra University, Visakhapatnam 530003, Andhra Pradesh, India; [d]Faculty of Medicine, Duy Tan University, Da Nang 550000, Vietnam

*Corresponding author:
Vinay Bharadwaj Tatipamula
Email: vinaybharadwajt@gmail.com; vinaybharadwajtatipamula@duytan.edu.vn
Mobile: +84-774562619
ORCID ID: http://orcid.org/0000-0002-9376-1911

The antioxidant and antidiabetic effects of sekikaic acid **(SA)** were investigated using *in vitro* and *in vivo* study models. **SA** possessed good antioxidant activity as assessed through hydroxyl radicals (IC_{50} value=41.5 µg/mL) and ferric ions assay (IC_{50} value=42.0 µg/mL). **SA** exhibited stronger α-glucosidase and α-amylase inhibition than that of aldose-reductase and protein tyrosine phosphatase 1B. The hypoglycemic activity of **SA** caused significant reduction of plasma glucose levels in normal and glucose loaded rats. The anti-hyperglycemic activity of **SA** (2 mg/Kg body weight) was indicated by the reduction of blood glucose by 44.17±3.78% in the third week in streptozotocin-induced diabetic rats. The hypolipidaemic action of **SA** was evident by the significant decrease in the levels of low-density lipoprotein, total cholesterol, and total glycerides. Histologically, the pancreas of the treated groups showed significant regeneration of the pancreatic β-cells compared to diabetic control, possibly due to the inhibition of digestive enzymes.

Keywords: *Dirinaria consimilis*, α-glucosidase, α-amylase, aldose-reductase, biochemical analysis, protein tyrosine phosphatase 1B, antidiabetic activity

Experimental Section

Material

Sekikaic acid **(SA)** was re-isolated according to the established procedures from lichens *Dirinaria consimilis* (Stirt.) D. D. Awasthi. Before biological analysis, compound **1** was purified by recrystallization technique using acetone and hexane (9:1) and finally, obtained as colorless crystals (450 mg, 0.23%w/w, based on total lichen material). Compound **1** was re-confirmed as sekikaic acid by using spectral analysis. Sekikaic acid **(1)**: Mol. For.: $C_{22}H_{26}O_8$; R_f: 0.6 (Dichloromethane:Ethyl acetate, 1:1); m.p: 220-221 ˚C; UV (methanol): λmax 219 nm; FT-MS-ESI (positive mode): 419.33 ($M\text{-}H^+$) (Figure S1-S4) (Tatipamula et al. 2019).

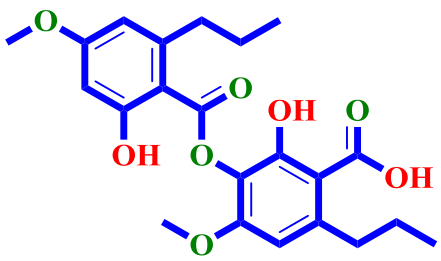

Figure S1. Chemical structure of sekikaic acid **(SA)**

Chemicals

All chemicals used in these experiments were of analytical grade. PYP IB, Streptozotocin (STZ), and Amylase HR reagent obtained from Himedia Laboratories Pvt. Ltd. (Mumbai, India) and Pro Lab Marketing Pvt. Ltd. (New Delhi, India), respectively. Intestinal acetone powders from rats purchased from Sigma Aldrich (Mumbai, India). Glibenclamide and rat feed procured from Avantis Pharma Ltd. (Mumbai, India) and Hindustan Lever Ltd. (Mumbai, India), respectively.

Antioxidant activity

Ferric ion (Fe^{3+}) reducing power assay

SA was exposed to Ferric ion (Fe^{3+}), reducing power assay in triplicate, and results were reported as inhibition level, % of Fe^{3+} ions (Haritha et al. 2019). To 2.5 mL phosphate buffer (pH 6.6, 0.2 M), added 2.5 mL potassium ferricyanide (1 %), and added know concentrations of

sample and incubated for 20 min. Later, to each sample, added 2.5 mL trichloroacetic acid (10 %) and 0.5 mL of ferric chloride (0.1 %) and observed absorbance at 700 nm against the blank. The IC_{50} value of **SA** was calculated by plotting concentrations against their inhibition level, %.

Hydroxyl radical assay

SA was exposed to hydroxyl free radicals assay in triplicate, and results were reported as inhibition level, % of hydroxyl free radicals (Talluri et al. 2018). Hydroxyl radicals were produced by reacting a solution of iron-EDTA with hydrogen peroxide. The generated hydroxyl free radicals were tested with known concentrations of samples, and incubated for 30 min at 37 ˚C, then added 2 mL of 2.8 % trichloroacetic acid, and thiobarbituric acid, boiled for 30 min and cooled, and noted absorbance at 532 nm. The IC_{50} value of **SA** was calculated by plotting concentrations against their inhibition level, %.

In vitro Antidiabetic activity

α-Glucosidase inhibitory assay

SA exposed to α-glucosidase inhibitory activity in triplicate, and results were reported as inhibition level, % of α-glucosidase (Tatipamula et al. 2019a). In 96 well microplate, take 2.0 µL of α-glucosidase, to it added 20 µL of know concentrations of the sample (25, 50, 75 and 100 µg/mL for **SA** or acarbose solubilized in DMSO) and 100 µL of 50 mM of pH 6.8 of phosphate buffer and incubated at 37 ˚C. Later, to each sample, added 50 µL of 5 mM of p-nitrophenyl-α-D-glucopyranoside (substrate) and incubated for 20 min. Then added 50 µL of 1 M of Na_2CO_3 and adjusted to 150 µL with pH 6.8 phosphate buffer and observed absorbance at 405 nm against the blank. The IC_{50} value of **SA** was calculated by plotting concentrations against their inhibition level, %.

Porcine pancreatic α-amylase

The assay of α-amylase inhibitory activity was estimated in a triplet (n = 3) (Tatipamula et al. 2019b). 100 µL of amylase HR reagent and 40 µL of the samples at different concentrations (25, 50, 75 and 100 µg/mL for **SA** or acarbose solubilized in DMSO) was added and incubated for 10 min at 37 ˚C. Then 60 µL of 0.1 mg/mL BPNPG7 (blocked p-nitrophenyl maltoheptaoside, was used as a substrate) in 0.1 M HEPES (4-(2-hydroxyethyl)-1-piperazineethanesulfonic acid) buffer of pH 6.9 was added to it and further incubated for 10 min at 37 ˚C and observed

absorbance at 700 nm against the blank. The IC_{50} value of **SA** was calculated by plotting concentrations against their inhibition level, %.

Aldose-reductase activity

SA subjected to aldose reductase activity in triplicate, and results were reported as inhibition level, % of aldose reductase (Talluri et al. 2018). The 10 % of homogenate (transparent eye lenses of normal albino rats) prepared with 0.1 M of pH 7.4 of phosphate buffer, centrifuged for 10 min, and the supernatant was isolated and stored in cold conditions. To 0.1 mL of the lens, supernatant added 0.7 mL of 0.067 M of phosphate buffer, 0.1 mL NADPH, 0.1 mL of 5×10^{-4} M substrate (DL-glyceraldehyde) except reference and adjust to 1 mL and observed absorbance at 340 nm against the blank. The IC_{50} value of **SA** was calculated by plotting concentrations against their inhibition level, %.

PYP IB enzymatic activity

SA subjected to PYP IB in triplicate, and results were reported as inhibition level, % of PYP IB (Song et al. 2017). The reaction mixture contains different concentrations of the test solution, 20 µL of 1 µg/mL of PYP IB, 40 µL of the substrate (p-nitrophenyl phosphate, 4 mM) in 130 µL of buffer (pH 7.5), and incubated for 10 min at 37 ˚C and observed absorbance at 405 nm against the blank. The IC_{50} value of **SA** was calculated by plotting concentrations against their inhibition level, %.

Animals

Albino rats (either sex, 50 in total) weigh 190-200 g, and albino mice (male, 5 in number) weigh 25-30 g were utilized for current experimental study. The experimental procedure was performed as per OECD regulations (Regd No. 516/01/A/CPCSEA) and approved by the Institutional Animal Ethics Committee of AU College of Pharmaceutical Science, Andhra University, Visakhapatnam with approval number as 516/PO/c/01/IAEC/17 dated 28 October 2019.

Toxicity studies

A week before the acute toxicity study, five male albino mice were kept on a standard diet under room temperature. Orally, **SA** at 20 mg/Kg body weight (b.w) was administered to the selected albino male mice (n = 5) and kept under observed for 14 days (Tatipamula et al. 2019c). The

mortality number triggered by **SA** within this time duration was observed, from which log dose-response plots were calibrated, and the median lethal dose (LD_{50}) of the sample was determined.

Hypoglycemic activity

Effect on normal or oral glucose loaded rats

SA was subjected to hypoglycemic activity by oral glucose tolerance (OGT) test (Tatipamula et al. 2019c). The levels of plasma glucose of overnight fasted normal albino rats were measured by using the tail vein puncture and glucometer method. Selected rats were grouped (n = 6) orderly and control group treated with 0.5 % CMC; the standard group with glibenclamide (1 mg/Kg b.w) and sample groups with **SA** at 1 and 2 mg/Kg b.w and observed plasma glucose levels at 0, 30 and 60 min, by using tail vein puncture method. At 60 min, all groups treated orally with 1.5 g/Kg glucose solution by using polyethylene gastric tube and observed plasma glucose levels at 120 and 240 min.

Anti-hyperglycemic activity

Induction of diabetes: Intraperitoneally STZ (55 mg/Kg b.w) was inducted to albino rats (overnight fasted), and rats were allowed to drink 0.5 g/Kg glucose solution (free access). Later, for three consecutive days, plasma glucose values of induced albino rats were observed, on the end of third-day rats with above 250 mg/dL plasma glucose value was segregated as diabetic and utilized for the experiment (Tatipamula et al. 2019c).

In vivo Antidiabetic activity: Selected albino rats were grouped (n = 6) orderly and control group treated with 0.5 % CMC; the standard group with glibenclamide (1 mg/Kg b.w) and sample groups with **SA** at 1 and 2 mg/Kg b.w. Initially, the groups were tested for one-day, later the therapy continued for 21 consecutive days, and the plasma glucose levels were measured on fasting at 1, 7, 14, and 21 day, simultaneously, the effect of body weight of albino rats was also observed. By piercing of retro-orbital plexus under diethyl ether (anesthesia), blood samples were collected from albino rats on 0th day and 22nd day, which was used for biochemical analysis include total cholesterol (TC), plasma triglyceride (TG), low and high-density lipoprotein (LDL and HDL) by using Randox diagnostic kits (Talluri et al. 2018; Tatipamula et al. 2017). Lastly, albino rats were sacrificed, and organs were detached for TBARS and histological studies.

Lipid Peroxidation (TBARS) in Tissues

The isolated organs, namely kidneys, liver, and pancreas, were washed with NaCl (0.9 %), homogenized by sucrose and centrifugation. To 0.2 mL homogenate added 1.5 mL acetic acid solution, 0.2 mL sodium dodecyl sulfate solution, and 1.5 mL thiobarbituric acid, and adjusted to 4.0 mL and boiled for 1 h. Later cooled, added 10 % trichloroacetic acid, and centrifuged 10 min and observed absorbance at 532 nm (Tatipamula et al. 2017).

Histopathological studies

The isolated pancreas was kept in saline and stored in formalin (10 %). By using a microtome, the pancreas was sliced to 5 μm sections and stained with hematoxylin and eosin.

Statistical analysis

All statistical analyses performed by using GraphPad Prism 5.0 (La Jolla, USA). The *in vitro* bioassays implemented in triplicate (n = 3), and the outcomes denoted as a mean±SD compared using one-way ANOVA followed by unpaired Student's t-test. While *in vivo* study results represented in mean ± SEM and statistical significance between the test groups denoted by one-way ANOVA followed by post-hoc Bonferroni. Differences within groups were related by using the unpaired and paired t-tests (2-tailed). The measured statistically significant *p*-value is lesser than 0.05.

Results

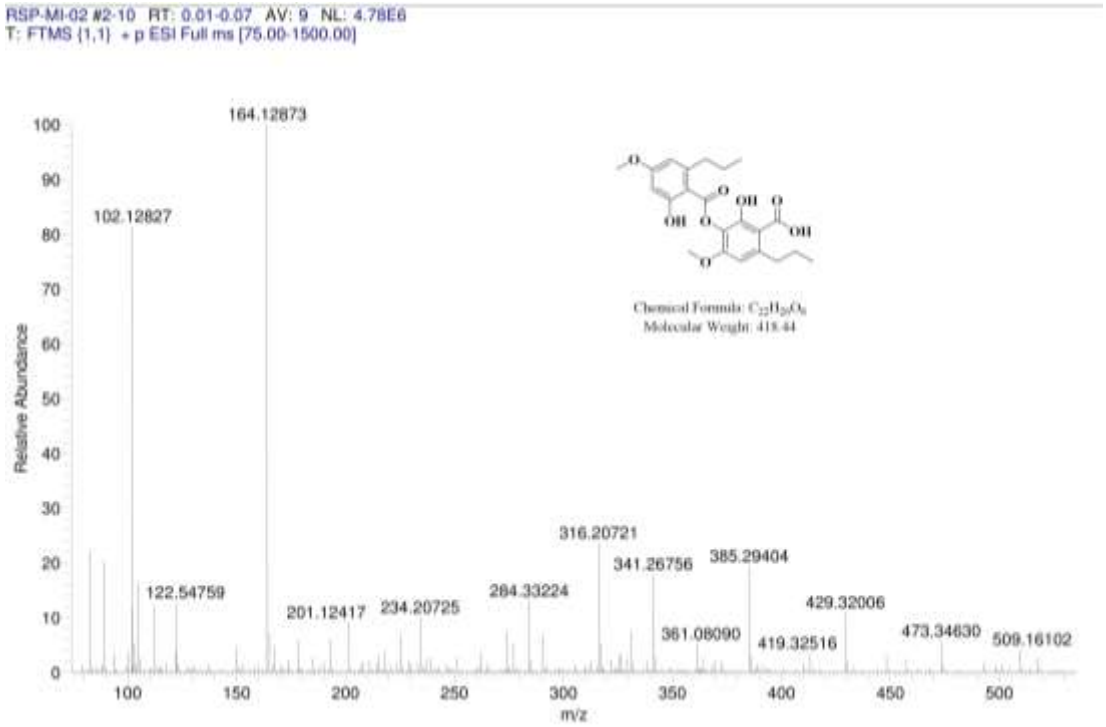

Figure S2. FT-MS-ESI positive mode spectrum of **SA**

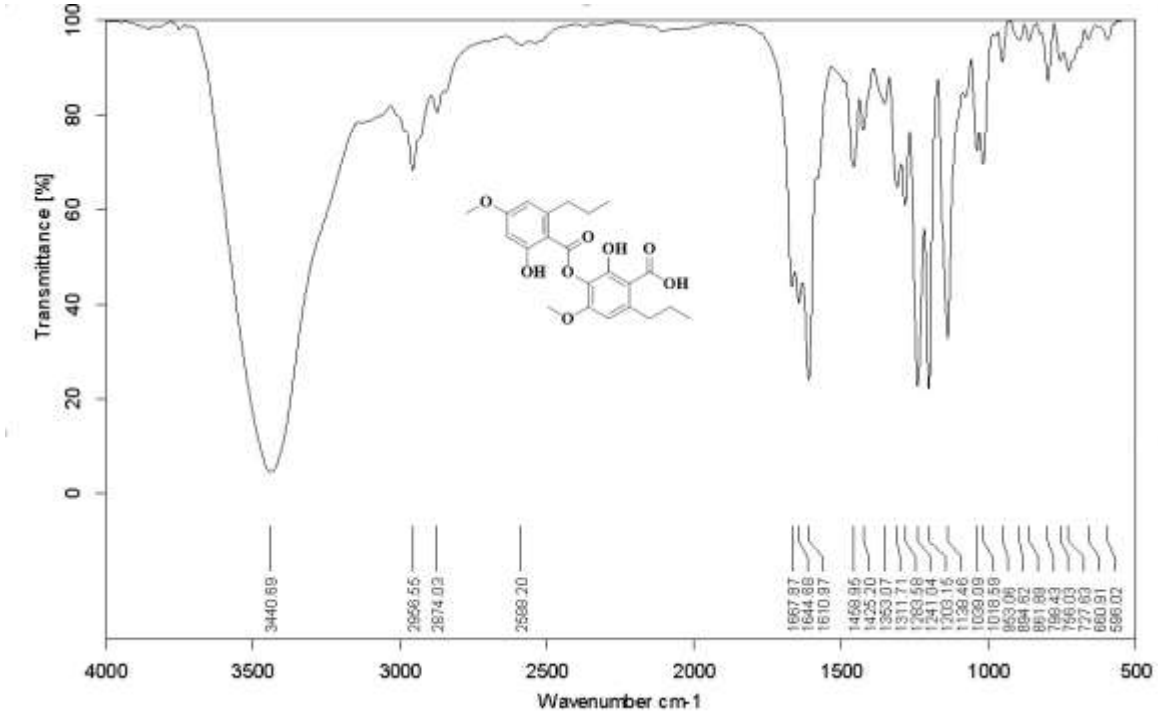

Figure S3. FT-IR spectrum of **SA** (KBr)

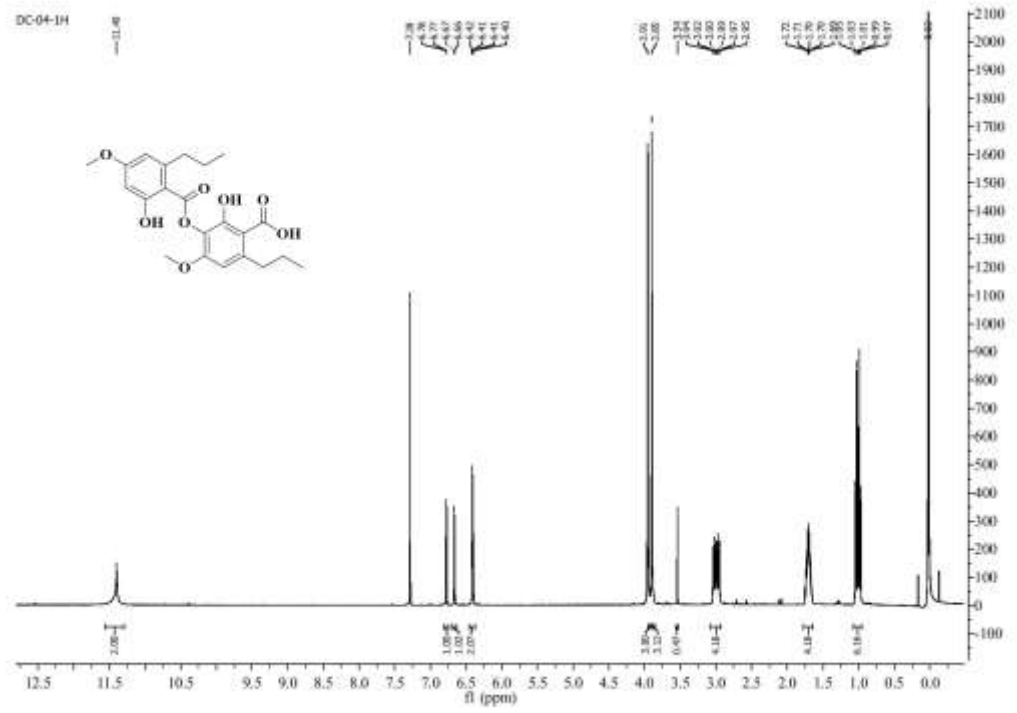

Figure S4. Proton NMR spectrum of **SA** ($CDCl_3$, 400 MHz)

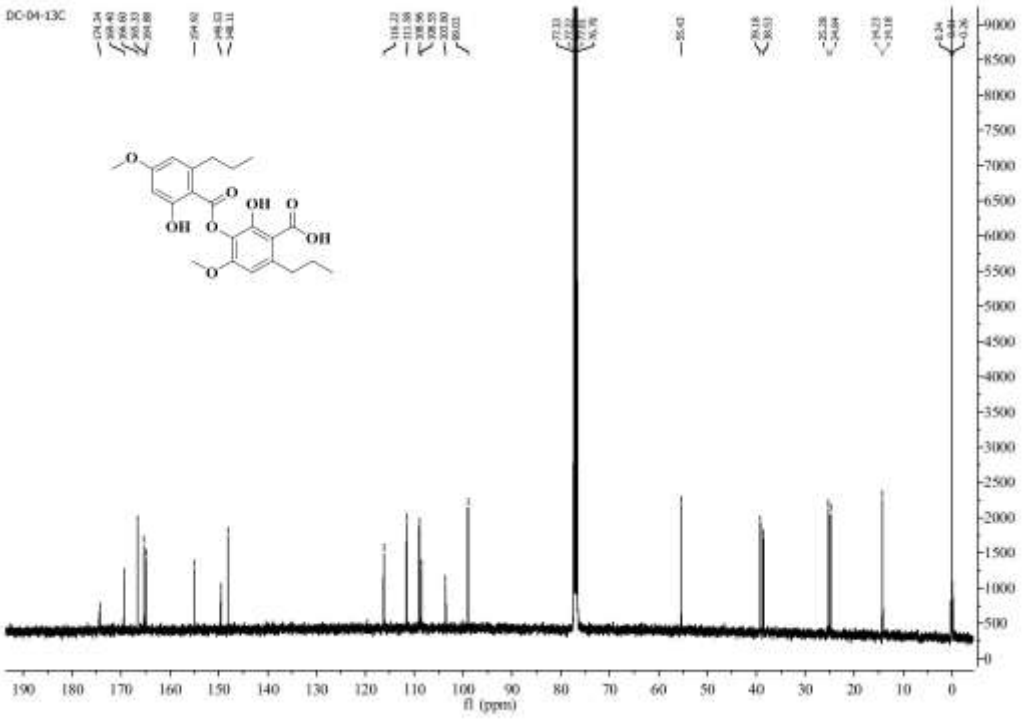

Figure S5. ^{13}C NMR spectrum of **SA** ($CDCl_3$, 400 MHz)

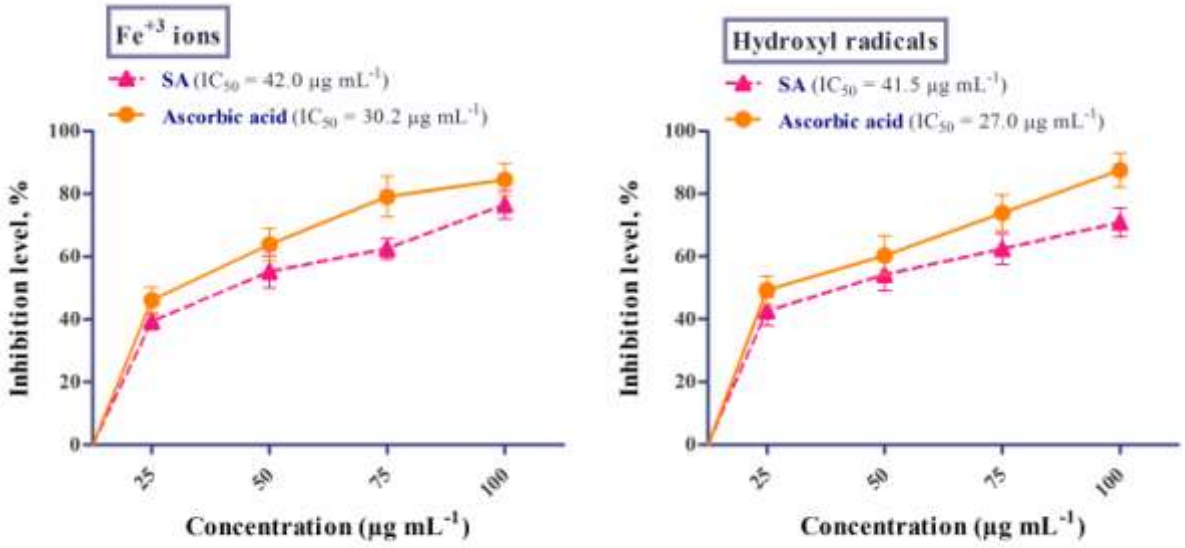

Figure S6. IC_{50} values of **SA** against ferric ions and hydroxyl radicals

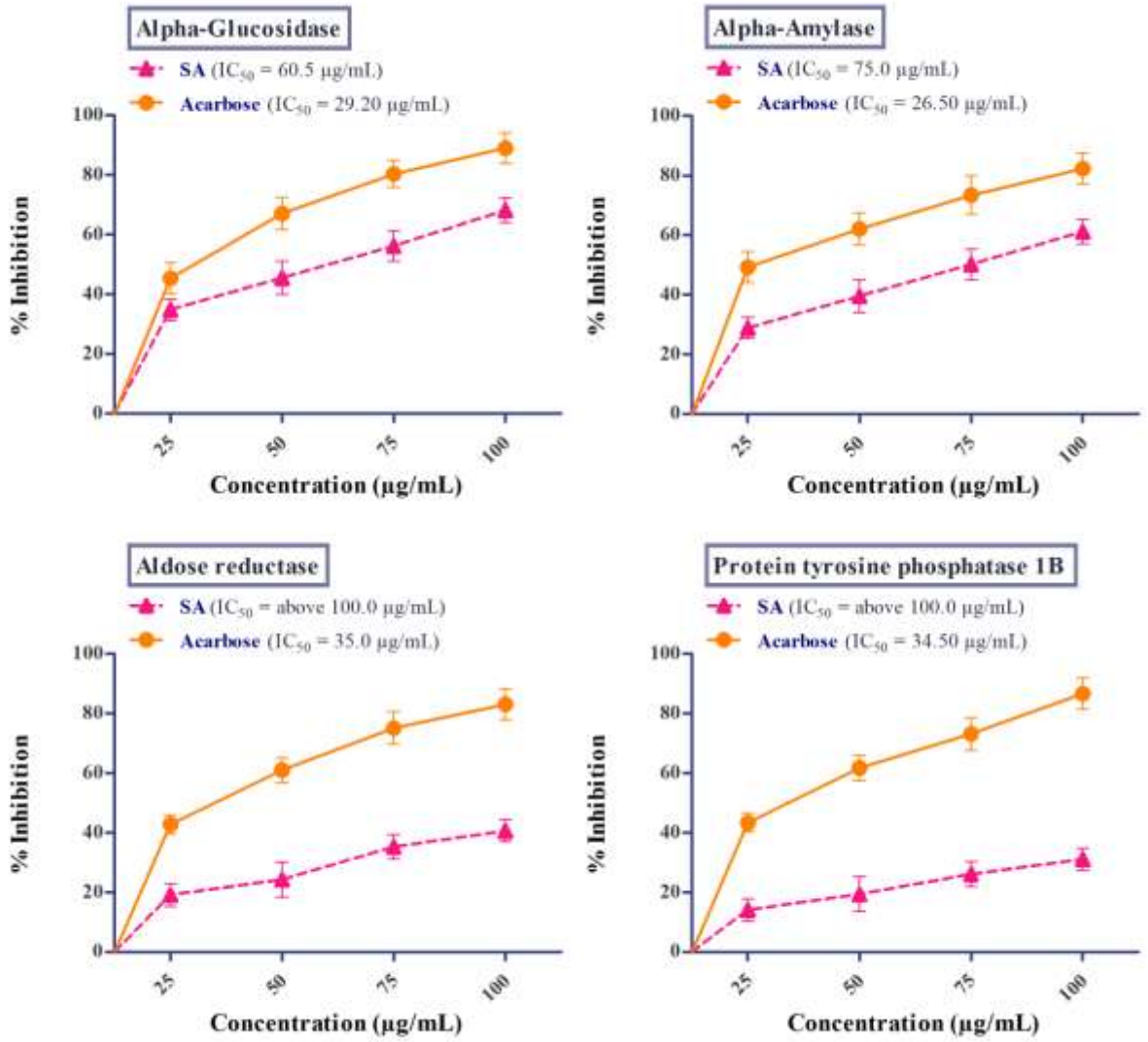

Figure S7. IC_{50} values of **SA** against α-glucosidase, α- amylase aldose reductase, and protein tyrosine phosphatase 1B enzymes

Table S1. *In vivo* hypoglycemic activity

Group	Plasma Blood Glucose level at different intervals of time (mg/dL)					
	0 min	**30 min**	**60+OGL min**	**90 min**	**120 min**	**240 min**
SA#	84.34±2.17	81.17±2.15*	79.17±3.12*	102.17±4.57	88.34±1.89*	93.17±2.07*
SA~	86.84±4.18	83.67±3.14*	80.34±3.54*	95.67±5.74	84.17±3.83*	78.17±3.04

Glibenclamide[#]	83.17±3.11	81.17±2.23*	75.50±2.01*	88.00±3.74	76.34±2.29*	64.84±2.06*
Control	86.67±3.02	85.50±5.32	84.34±3.08	112.50±3.57	135.17±5.02	152.84±5.91

[#]1 mg/Kg body weight; ˜2 mg/Kg body weight; Values are mean±SEM of six rats per group, *statistically between the test groups denoted by one-way ANOVA followed by post-hoc Bonferroni. Differences within groups were related by using the unpaired and paired t-tests (2-tailed) with $p<0.05$

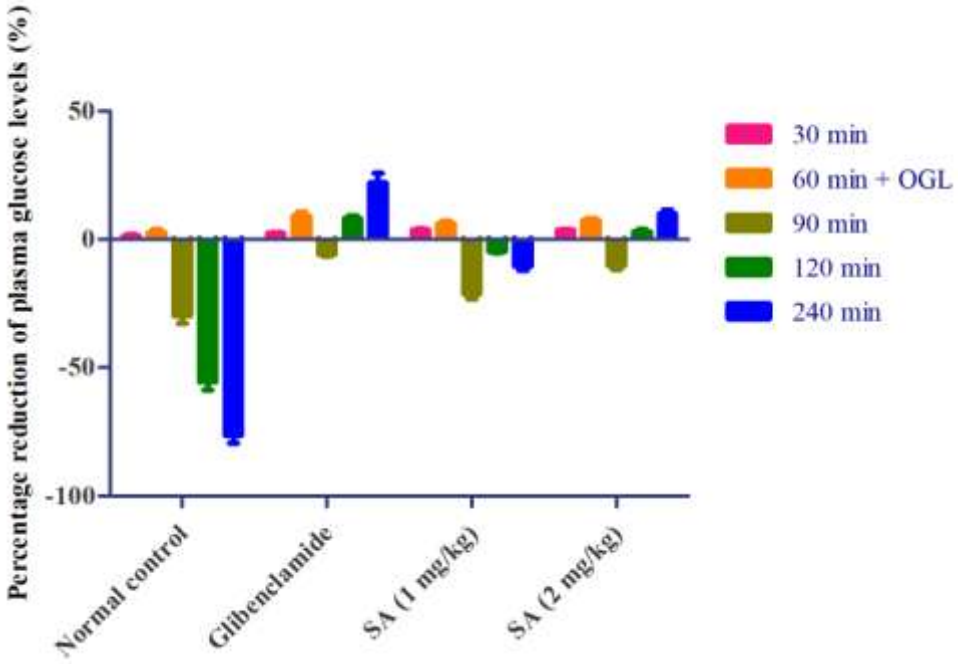

Figure S8. Percentage variation of plasma blood glucose levels in normal and glucose loaded albino rats

Table S2. Variation of plasma blood glucose levels in STZ-induced diabetic albino rat within 21 days of treatment

Group	**Plasma Blood Glucose level at different intervals of time (mg/dL)**			
	0 day	**7 day**	**14 day**	**21 day**
SA[#]	358.00±4.07	327.67±8.04	294.84±8.65	280.84±9.50
SA[˜]	350.17±3.80	298.67±6.80*	261.00±5.31*	195.50±6.70
Glibenclamide[#]	367.50±6.30	280.67±6.00*	221.34±5.12*	160.67±6.14*

Diabetic Control	348.14±7.90	377.34±6.30	389.84±6.87	393.67±7.67
Control	93.67±5.67	96.34±3.62	97.84±2.56	98.50±5.01

[#]1 mg/Kg body weight; ˜2 mg/Kg body weight; Values are mean±SEM of six rats per group, *statistically between the test groups denoted by one-way ANOVA followed by post-hoc Bonferroni. Differences within groups were related by using the unpaired and paired t-tests (2-tailed) with $p<0.05$

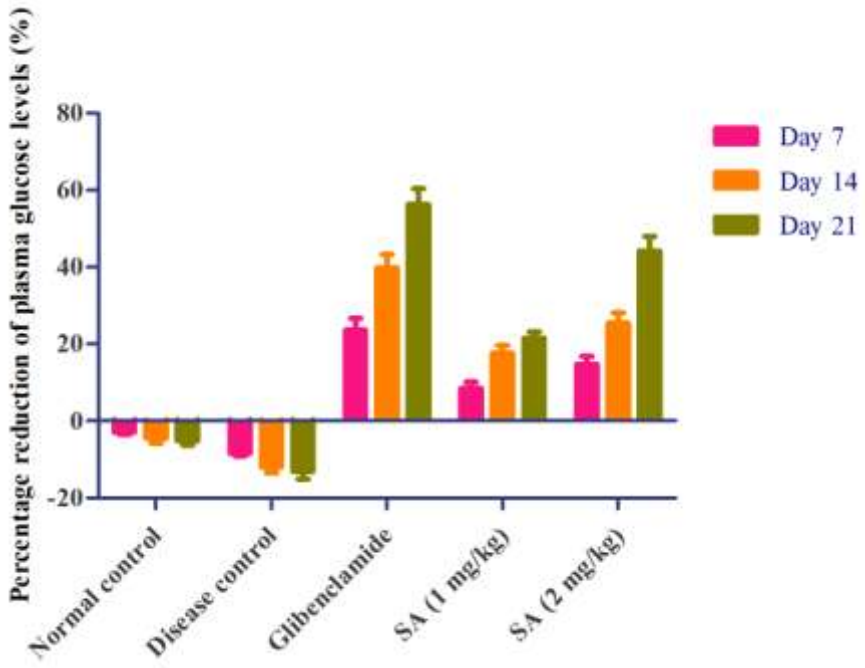

Figure S9. Percentage variation of plasma blood glucose levels in STZ-induced albino rats within 21 days of treatment in all groups

Table S3. Variation of body weight in STZ-induced diabetic albino rat within 21 days of treatment

Group	**Body weight at different intervals of time (mg/dL)**			
	0 day	**7 day**	**14 day**	**21 day**
SA[#]	196.00±6.12	197.84±6.02	194.17±5.41*	190.67±7.41
SA˜	198.17±6.22	203.17±6.72	201.34±4.95*	205.50±7.17*
Glibenclamide[#]	200.50±5.25	205.67±5.60*	211.50±3.63*	215.84±4.17*

Diabetic Control	202.34±6.18	192.34±6.82	182.67±5.58	178.17±7.68
Control	201.67±7.20	200.50±8.21	209.84±8.36	220.34±5.88

[#]1 mg/Kg body weight; ˜2 mg/Kg body weight; Values are mean±SEM of six rats per group, *statistically between the test groups denoted by one-way ANOVA followed by post-hoc Bonferroni. Differences within groups were related by using the unpaired and paired t-tests (2-tailed) with $p<0.05$

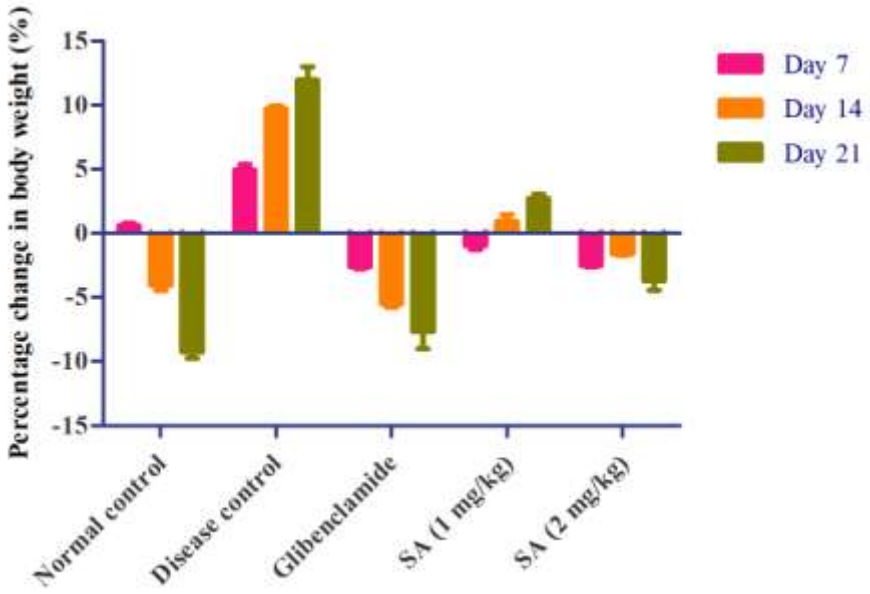

Figure S10. Percentage variation of body weight within 21 days of treatment in all groups

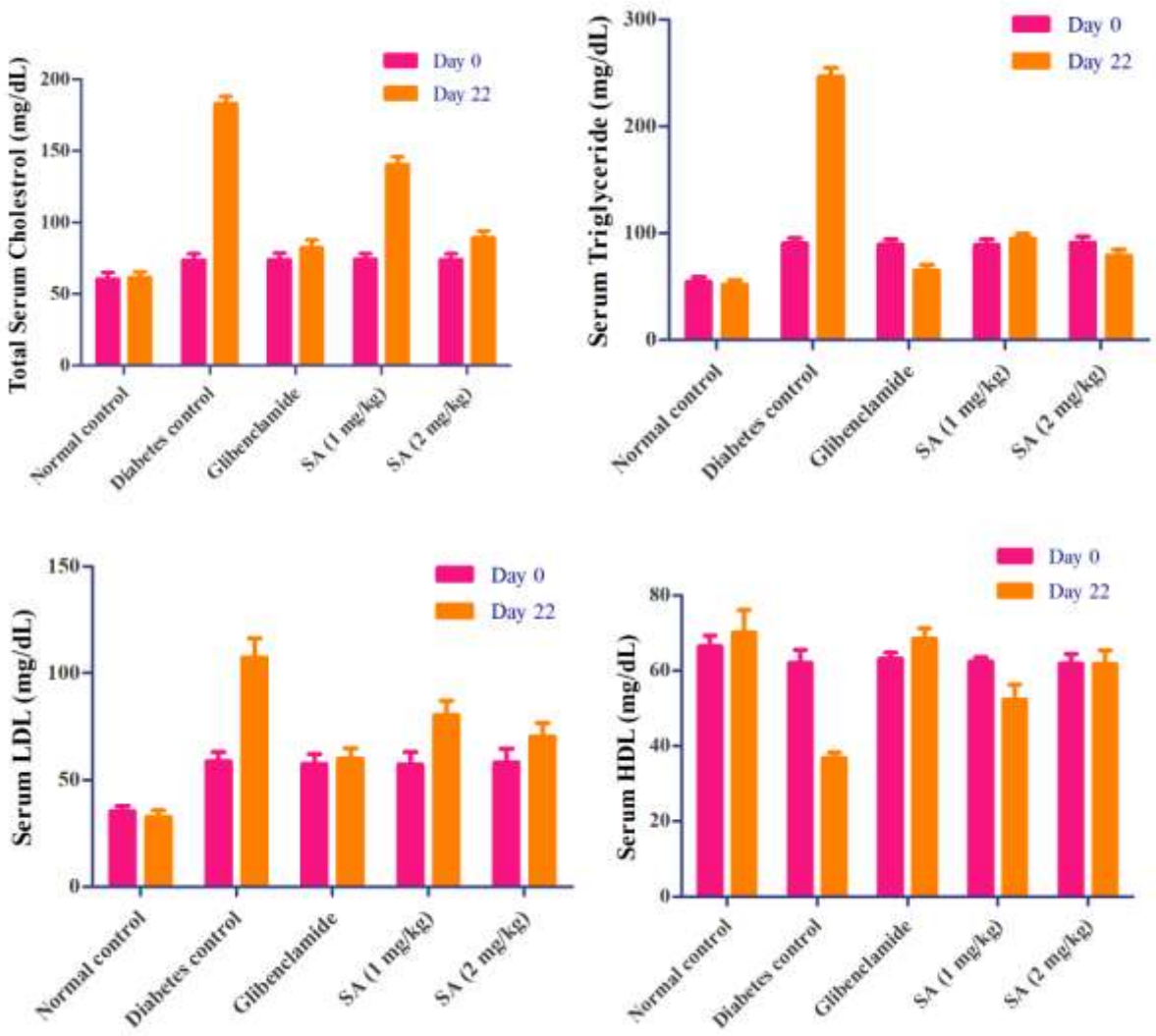

Figure S11. Effects of **SA** on serum total cholesterol (TC), triglycerides (TG), High-density lipoprotein (HDL), and low-density lipoprotein (LDL) levels after 21 days of treatment in all groups

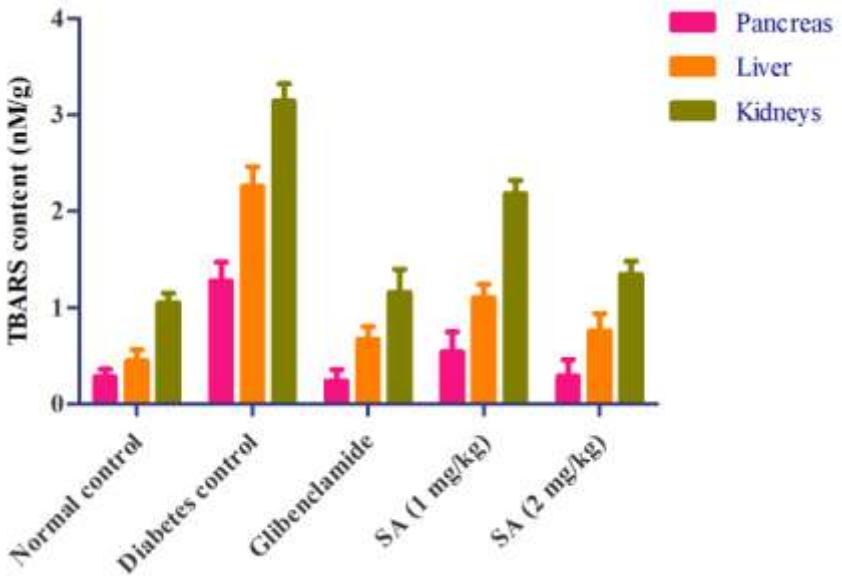

Figure S12. TBARS levels in the pancreas, liver, and kidneys after 21 days of treatment in all groups

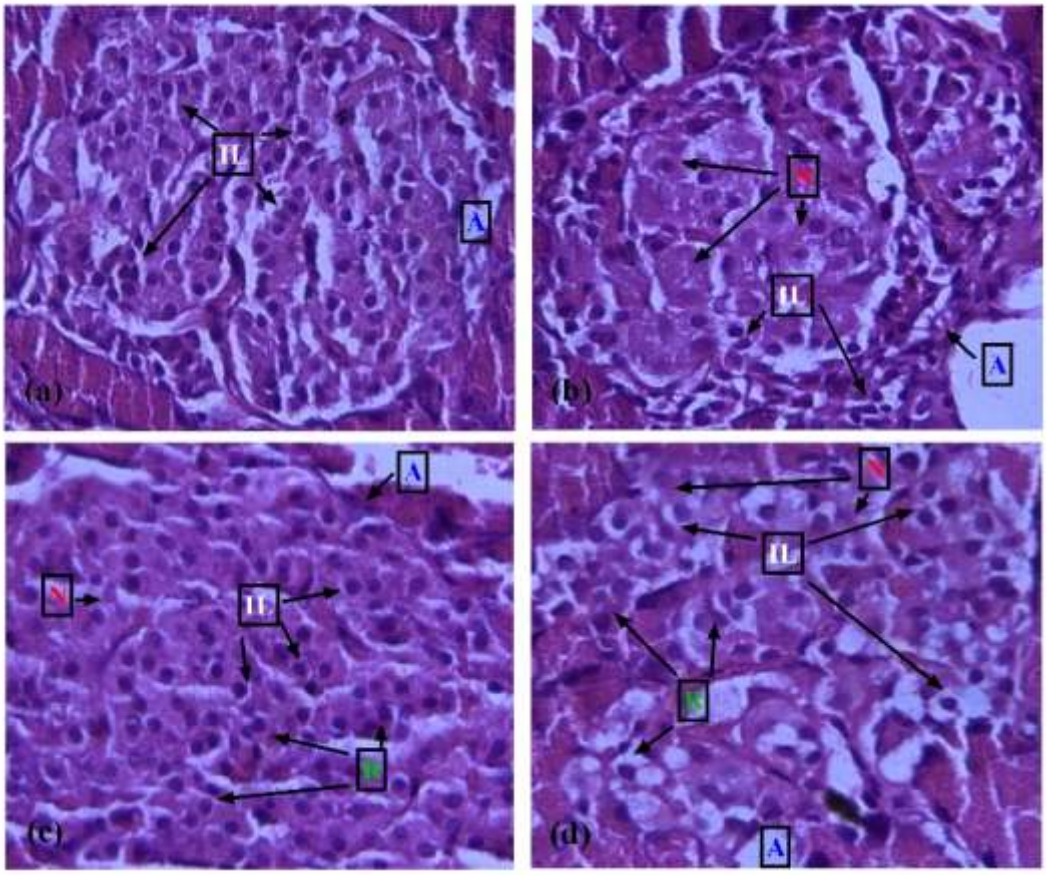

Figure S13. Histopathological study of pancreatic tissues in rats **(a)** Normal Control pancreas; **(b)** Diseased pancreas; **(c)** Glibenclamide treated pancreas at 1 mg/Kg b.w; **(d) SA** treated pancreas at 2 mg/Kg b.w

(A. acini; IL. islets of Langerhans; N. necrosis, R. regeneration)

Table S4. Summary of histological changes in the pancreas

Group	**Histopathological features of pancreatic damage**			
	Necrosis of Langerhans islets	Depletion of Langerhans islets	Regenerated Langerhans islets	Acini damage
Normal Control	-	-	-	-
Diabetic Control	+++	+++	-	+++
SA (2 mg/Kg b.w)	+	+	++	-
Glibenclamide (1 mg/Kg b.w)	-	+	+++	-

Keys: - (none); + (mild); ++ (moderate); +++ (severe)

References

Haritha P, Patnaik SK, Tatipamula VB. 2019. Chemical and pharmacological evaluation of manglicolous lichen Graphis ajarekarii Patw. & CR Kulk. Vietnam Journal of Science and Technology. 57:300-308.

Song YH, Uddin Z, Jin YM, Li Z, Curtis-Long MJ, Kim KD, Cho JK, Park KH. 2017. Inhibition of protein tyrosine phosphatase (PTP1B) and α-glucosidase by geranylated flavonoids from Paulownia tomentosa. J Enzyme Inhib Med Chem. 32:1195-1202.

Talluri MR, Ketha A, Battu GR, Swamy R, Tatipamula VB. 2018. Protective effect of Aurelia aurita against free radicals and streptozotocin-induced diabetes. Bangladesh J Pharmacol. 13:287-295.

Tatipamula VB, Killari KN, Ketha A, Sastry VG. 2017. Taxithelium napalense acts against free radicals and diabetes mellitus. Bangladesh J Pharmacol. 12:197-203.

Tatipamula VB, Vedula GS, Sastry AVS. 2019. Antarvediside A-B from manglicolous lichen Dirinaria consimilis (Stirton) D.D. Awasthi and their pharmacological profile. Asian J Chem. 31:805-812.

Tatipamula V, Killari K, Gopaiah K, Alekhya K. 2019a. GC-MS Analysis of ethanol extract of Taxithelium napalense (Schwaerg) Broth along with its α-glucosidase inhibitory activity. Indian J Pharm Sci. 81:569-574.

Tatipamula VB, Haritha P, Rao GSNK, Alekhya K, Yejella RP. 2019b. Isolation and characterization of metabolites from Clathria procera Ridley extract and evaluation of its antidiabetic effects in Streptozotocin-induced diabetic rats. Journal of Experimental and Applied Animal Sciences. 3:35-56.

Tatipamula VB, Kolli MK, Lagu SB, Paidi KR, Reddy R, Yejella RP. 2019c. Novel indolizine derivatives lowers blood glucose levels in Streptozotocin-induced diabetic rats: A histopathological approach. Pharmacol Rep. 71:233-242.